First-Principles Study of Electronic and Magnetic Properties of Co_nMn_m and Co_nV_m ($m + n \leq 6$) Clusters

Pan Wu, Lan-Feng Yuan,* and Jinlong Yang

Hefei National Laboratory for Physical Sciences at Microscale, University of Science and Technology of China, Hefei, Anhui 230026, People's Republic of China

Received: May 12, 2008; Revised Manuscript Received: September 23, 2008

The electronic and magnetic properties of small Co_nMn_m and Co_nV_m ($m + n \leq 6$) clusters are systematically studied using density functional theory. The results show that Co and V atoms prefer to aggregate in Co−Mn and Co−V clusters, respectively. Significant magnetic moment enhancement in Co−Mn clusters with Mn doping and reduction in Co−V clusters with V doping are found, consistent with experiment results for larger clusters [*Phys. Rev. Lett.* **2007**, *98*, 113401]. The results are discussed by analyzing the magnetic coupling type and local magnetic moment on each atoms. Density of states and vertical ionization potentials are calculated and show cluster size dependent behavior.

I. Introduction

Clusters are attractive for their novel properties different from conventional bulk ones, because of their small sizes and large surface effects. The magnetic properties of transition metal clusters are much more interesting than those of their bulks for their promising application on higher storage densities in magnetic memory. Many experimental groups have found that the magnetic moments per atom of Fe, Co, and Ni clusters are significantly larger than their corresponding bulk values,[1,2] and nonvanishing magnetic moments are discovered in some transition metal clusters which are not magnetic in their bulk states.[3,4] Bimetallic clusters have recently been reported as having even more interesting effects. The transition from ferromagnetic (FM) to antiferromagnetic (AFM) coupling was found in the Cr−Fe bimetallic clusters with increase of Cr.[5] Many investigations in cobalt mixed 4d transition metal clusters have been reported to study the interaction of 3d electrons with 4d electrons, such as Co−Rh[6−8] and Co−Pd.[9,10] Recently Yin et al. conducted experiments for Co_nMn_m and Co_nV_m clusters ($n \leq 60$, $m \leq n/3$)[11] and found significant magnetic moment enhancement with doped Mn and reduction with doped V. They gave a qualitative explanation based on the formation of virtual bond states (VBS). On the other hand, as they pointed out, theoretical investigations using more advanced tools would definitely shed more lights on the mechanism and elucidate more details. As we know, there is no systematic theoretical study for small Co−Mn and Co−V clusters yet. In this article, we carry out first-principles investigations on Co_nMn_m and Co_nV_m ($m + n \leq 6$).

II. Computational Methods

Even though we limit ourselves in clusters within 6 atoms, there are still many different structures to consider, and the number of candidates grows fast with the cluster size. Therefore, we have adopted a method which maximizes our chance to find the ground-state structures. This method includes three steps.

First, for each specific atom number, we choose various reasonable initial structures. These initial structures are ground-state and low-lying structures for the pure clusters of Co, Mn, and V, according to either our calculations or literature on these pure clusters.[12−18] For example, for 3-atom clusters we consider linear and triangular structures and for 4-atom clusters rhombic and tetrahedral.

Second, based on these initial structures, we try different compositions and positions on them for both the systems of Co−Mn and Co−V. For example, from the linear initial structure of 3-atom clusters, we get 6 candidates for Co−Mn: 1 for Co_3, 2 for Co_2Mn, 2 for $CoMn_2$, and 1 for Mn_3. In this way, we have considered more than two hundred candidates altogether.

Third, after all of the candidates are optimized, we implement frequency analysis on the structures with the lowest energies to make sure that they are indeed stable structures.

Our calculations are carried out using density functional theory (DFT) implemented in the DMol^3 package.[19] We perform all-electron spin-unrestricted calculations with scalar relativity (via VPSR tag), using double numerical plus polarization basis set (DNP)[19] and the Perdew−Burke−Ernzerhof (PBE)[20] functional within generalized gradient approximation (GGA). The direct inversion in iterative subspace (DIIS) approach is used to speed up SCF convergence. The grid for numerical integration is set as "fine". The atomic distance cutoff in real space is 5.5 Å. The convergence criteria for energy, energy gradient, and displacement are 1×10^{-5} Hartree, 2×10^{-3} Hartree/Å, and 5×10^{-3} Å, respectively. The optimized structures for all of the Co_nMn_m and Co_nV_m ($m + n \leq 6$) clusters are shown in the Figures 1 and 2.

The binding energy of a given cluster is defined as the total energy of the cluster minus the sum of reference energies of free atoms. The reference energy of each atom is calculated by spin-unrestricted method. For Co and Mn, we take their configurations as $3d^74s^2$ and $3d^54s^2$, which are the lowest energy configurations of these two atoms in our calculations, consistent with the Hund rule. While for V, we choose the $3d^44s^1$ configuration (not the true lowest energy configuration $3d^34s^2$), as proposed by Baerends,[21] and it is the lowest energy configuration for V within our method. In some conditions the

* To whom correspondence should be addressed. E-mail: yuanlf@ustc.edu.cn.

10.1021/jp804188u CCC: $40.75
Published on Web 11/08/2008

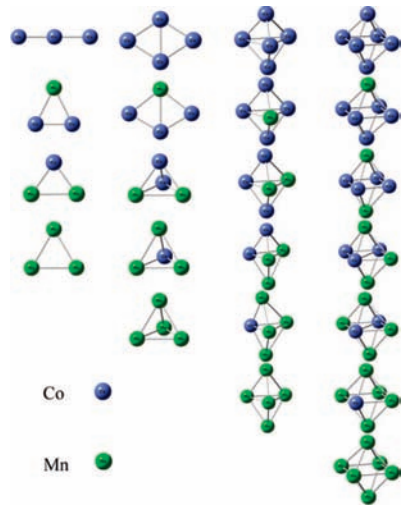

Figure 1. Ground-state structures of Co_nMn_m ($m + n \leq 6$).

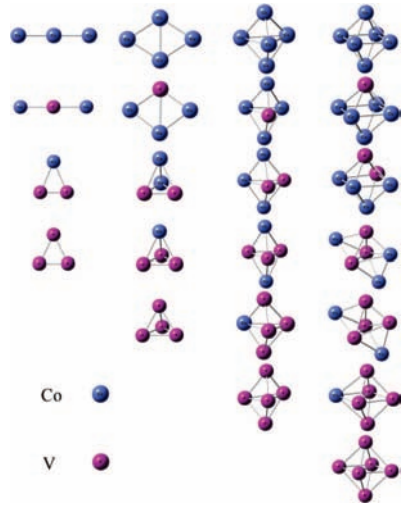

Figure 2. Ground-state structures of Co_nV_m ($m + n \leq 6$).

binding energy per atom is more useful, and we name it as average binding energy (ABE). The ABE graph is shown in Figure 3.

The magnetic moment is taken as the net spin, i.e., majority spin minus minority spin. The charge population at each atomic orbital is obtained by Mulliken analysis. The magnetic moments per atom, or average magnetic moments (AMM), are shown in Figure 4.

III. Optimization Results

A. $m + n = 2$. To validate the reliability of the present calculation, we first compare our calculation results with previous reports on the pure dimers of Co, Mn, and V. Table 1 presents their equilibrium bond lengths, binding energies, and magnetic moments. As we see, all of these properties are in good agreement with former experiments and calculations.

An interesting case is the calculated binding energy of Co_2 in literature: Ma et al. got a result of -5.08 eV,[12] apparently very far from the experimental value -1.72 eV.[22] However, the match may be not as poor as it looks. Since Ma et al. also used the DMol[3] program, it is very possible that they directly extracted the binding energy from the output for Co_2. Actually, their -5.08 eV is close to the raw output -4.99 eV in our calculation. But after manually subtracting twice the reference energy of $3d^74s^2$ Co atom from the total energy of Co_2, we get -1.76 eV, which then agrees quite well with the experimental value. The importance of checking the atomic reference energy is highlighted by this example!

As a general trend for dimers, intermetallic Co−Mn/V bond length is between the corresponding values for the pure clusters: Co−Mn bond length is 2.41 Å, between 2.11 Å for Co−Co and 2.59 Å for Mn−Mn; Co−V bond length is 2.08 Å, between 2.11 Å for Co−Co and 1.80 Å for V−V. The binding energies of V−V, V−Co, Co−Co, Co−Mn, and Mn−Mn are -2.69, -2.31, -1.76, -1.57, and -0.76 eV, respectively. It is clear that the binding strengths for dimers follow this rule: V−V > V−Co > Co−Co > Co−Mn > Mn−Mn.

B. $m + n = 3$. Structures of pure clusters Co_n, Mn_n, and V_n ($3 \leq n \leq 6$), as we obtained, are consistent with former reports.[13,23,24] Co_3 cluster favors linear structure. But as the Mn or V doping increases, the triangular structure becomes ground state. ABE changes with doped Mn/V in a monotonic increasing/decreasing trend. For Co_nMn_m, the difference of ABE between $CoMn_2$ and Mn_3 (about 0.30 eV) is much larger than that of $Co_2Mn-CoMn_2$ (0.13 eV) and Co_3-Co_2Mn (0.13 eV).

C. $m + n = 4$. Co_4 and Co_3TM (TM = Mn and V) clusters favor planar structures. Other four-atom clusters adopt three-dimensional structures. The structures of Co_nMn_m and Co_nV_m with the same m value are similar.

D. $m + n = 5$ and 6. Although we have tried 3 kinds of initial structures C_{5v}, D_{4h}, and D_{3h} for 5-atom clusters, after optimization every ground-state goes to D_{3h}-like. Most of the structures for Co_nMn_m and Co_nV_m with the same m value are similar, except Co_2Mn_3 and Co_2V_3: in Co_2Mn_3 the two Co atoms bond together, while in Co_2V_3 the two Co atoms are separated by three V atoms. In the 6-atom clusters, different structures between two systems with the same m appear as $m = 2-4$. In Co_4Mn_2, the two Mn atoms are separated by the Co plane; while in Co_4V_2, the two V atoms are bonded together. Co_3Mn_3 and Co_2Mn_4 are D_{4h}-like, whereas Co_3V_3 and Co_2V_4 are C_{2v}-like.

IV. Discussion

A. Aggregation Effect and Binding Energy. We can understand the above differences between Co_nMn_m and Co_nV_m in terms of aggregation effects: Co atoms congregate in Co_nMn_m, while V atoms congregate in Co_nV_m. For example, in Co_4Mn_2, the two Mn atoms lie on two sides of the Co plane, whereas in Co_3V_3 and Co_2V_4, the Co atoms are separated by V. The aggregation effect may be attributed to the order of bond strengths as in subsection III.A: V−V > V−Co > Co−Co > Co−Mn > Mn−Mn, which can also be extracted from the ABE plotted in Figure 3.

Because of the bond strength order, the Co_nMn_m clusters tend to create the largest number of Co−Co bond, then Co−Mn bond, and then Mn−Mn bond. The same kind of effect in Co−V clusters makes V aggregated and Co segregated by V. Also because of the bond strength order, Co_nMn_m/Co_nV_m exhibits increasing/decreasing trend for ABE with increasing m. If we assume the binding energy of each bond type is constant, then we can fit all the binding energy data to get a set of average results in these clusters. The fitted bond energies are -1.30, -1.25, -1.13, -1.00, and -0.73 eV for V−V, V−Co, Co−Co, Co−Mn, and Mn−Mn, respectively. They have the same trend as that in dimers, while being smaller (in absolute value) than those of dimers. This is reasonable, because, with the increase of cluster size, in general the "bonding ability" of each atom is partitioned to more bonds, and each bond becomes weaker.

In the dimers' binding energies, the difference between Co−Co and Co−Mn is only 0.19 eV, much smaller than any

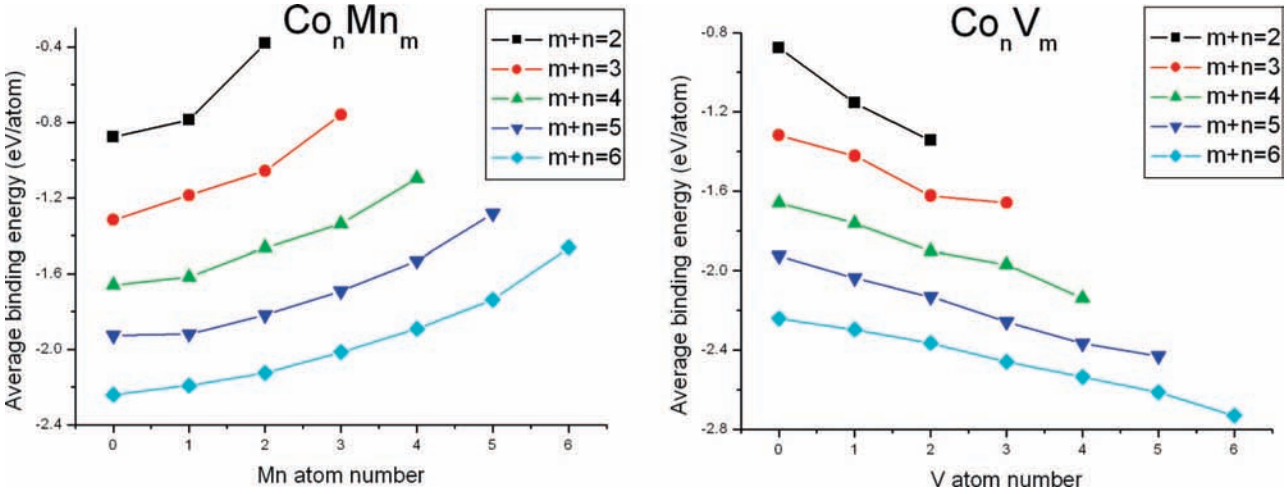

Figure 3. Average binding energy of Co_nTM_m (TM = Mn and V, $m + n \leq 6$).

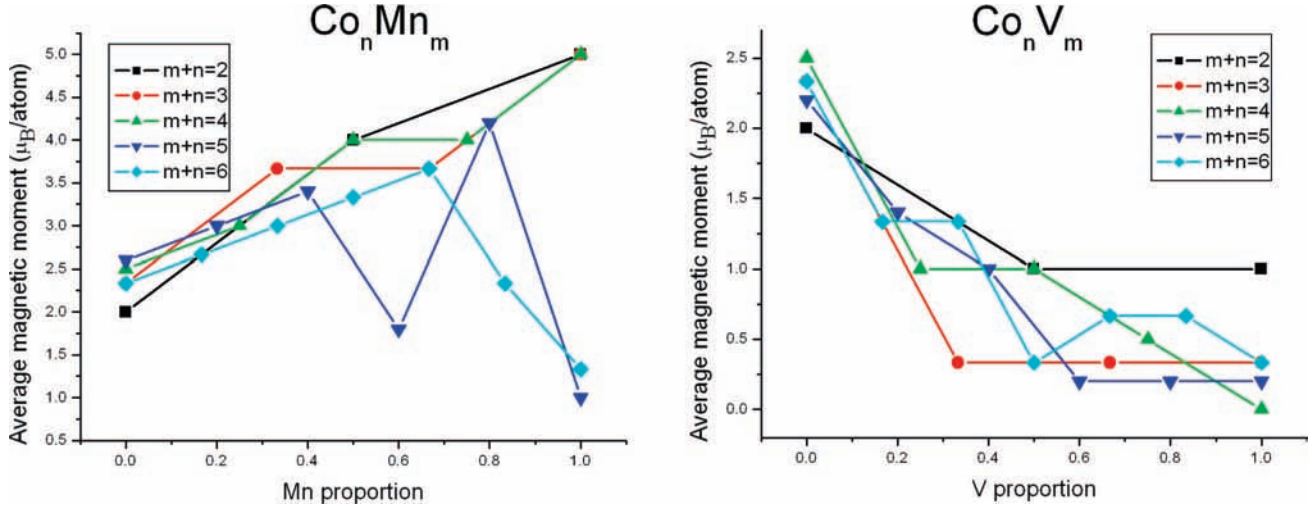

Figure 4. Average magnetic moment of Co_nTM_m (TM = Mn and V, $m + n \leq 6$).

TABLE 1: Bond Lengths (Å), Binding Energies (eV), and Magnetic Moments (μ_B) of Co, Mn, and V dimers

dimer		bond length	binding energy	magnetic moment
Co_2	present work	2.112	−1.76 (−4.99 [a])	4
	other theory[12]	2.144	−5.08[a]	4
	experiment[22]	2.31	−1.72	4
Mn_2	present work	2.59	−0.76	10
	other theory[23]	2.6	−0.98	10
V_2	present work	1.801	−2.69	2
	other theory[25]	1.802	−2.77	2
	experiment[26,27]	1.77	−2.75	N/A

[a] Directly extracted from DMol[3], without correction due to the reference energy of Co.

TABLE 2: Local Magnetic Moment (μ_B) in Co_5TM and $CoTM_5$ (TM = Mn and V)

		local magnetic moment	
system		TM = Mn	TM = V
Co_5TM	Co	2.29	1.90
	Co	2.29	1.90
	Co	2.32	2.42
	Co	2.29	2.11
	Co	2.29	2.11
	TM	4.52	−2.44
$CoTM_5$	Co	1.90	2.02
	TM	4.17	−0.59
	TM	4.17	1.01
	TM	4.17	−0.59
	TM	−4.57	1.08
	TM	4.17	1.08

other difference. Therefore, it is not shocking to see that there are two exceptions for the above rule of aggregation in Co−Mn systems: Co_3Mn_2 and Co_2Mn_4. Anyway, our research about the small bimetallic cluster can indicate a trend for the aggregation effect. This effect may become more prominent with the increase of cluster size.

For pure clusters, ABE decreases with the increase of atom number, i.e., the stability of system is strengthened. This effect is easily understood because of the increasing number of bonds per atom. An interesting phenomenon is found in Co_nMn_m: The difference of ABE for Mn_m−$CoMn_{m-1}$ is larger than those of all of the other Co_kMn_{m-k}−$Co_{k+1}Mn_{m-k-1}$, $1 \leq k \leq m - 1$. This implies that the stability of pure Mn clusters can be largely enhanced by doping a small amount of cobalt.

B. Magnetic Property. For Co_nMn_m, the AMM increases with doped Mn when m is not large. By multiplying the AMM with $m + n$, we get the total magnetic moment. It increases by about $2\mu_B$ per Mn atom doping as m is small, but when m gets large, it decreases rapidly. This result is consistent with the experimental results for larger clusters that the total magnetic moment enhancement with substitution of one Co atom by Mn is $1.7\mu_B$, and the increasing trend only persists for Mn

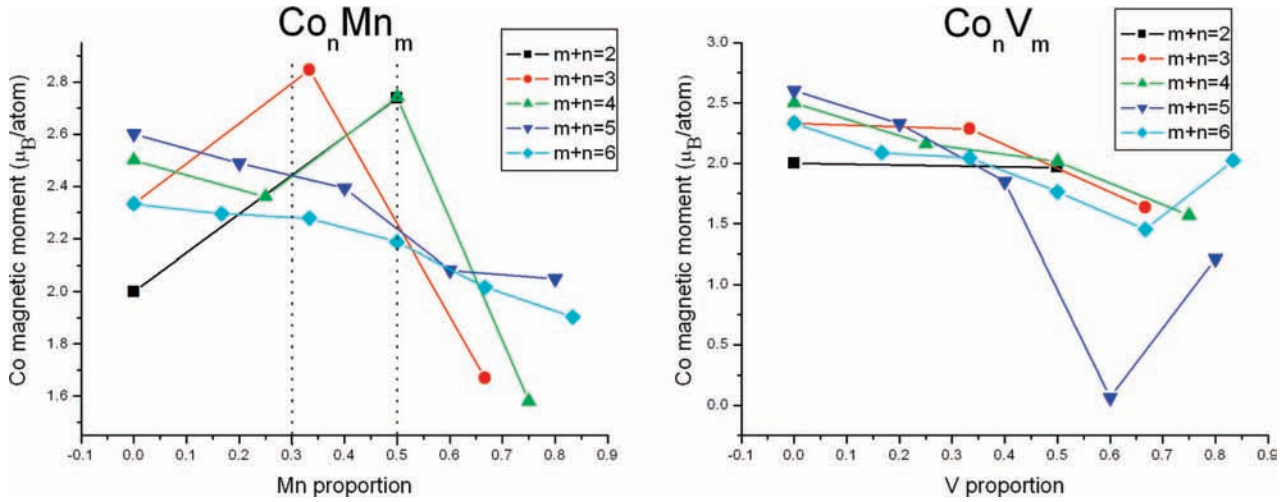

Figure 5. Average local magnetic moment of cobalt in Co_nTM_m (TM = Mn and V, $m + n \leq 6$).

TABLE 3: Co 3d Occupation Number and 3d Magnetic Moment (μ_B) in Co_m Mn_n ($m + n = 4$)

system	occupation	magnetic moment
Co_4	7.66	2.22
Co_3 Mn	7.67	2.20
Co_2 Mn_2	7.64	2.23
$CoMn_3$	7.99	1.78

TABLE 4: Co 3d Occupation Number and 3d Magnetic Moment (μ_B) in Co_m V_n ($m + n = 4$)

system	occupation	magnetic moment
Co_4	7.66	2.22
Co_3 V	7.77	1.84
Co_2 V_2	7.82	1.81
CoV_3	7.95	1.52

concentrations up to 30% to 40%, after which the magnetic moment decreases with increasing Mn concentration.[11]

The basic trend for V doped Co is as follows: with increase of m, total magnetic moment drops by $6\mu_B$ per V atom, until that is not much larger than $6\mu_B$. This is consistent with the experimental result that doping V atoms in Co clusters reduces the magnetic moment by about $6\mu_B$ per V.[11]

Why do Co−Mn and Co−V have different trends? From the Mulliken analysis of different atoms' local magnetic moment (refer to Table 2), we find out the reason. In Co_nMn_m, the local magnetic moments are as large as nearly $2.0\mu_B$ and $4.5\mu_B$ for Co and Mn, respectively. When Mn concentration is small, the Mn atoms are separated by Co atoms, and Mn−Co couple in a FM way; therefore, the AMM increases with Mn proportion. But when there are so many doped Mn atoms that they get together, the AFM coupling among Mn−Mn, as in bulk state, makes the AMM decreased. It is the same effect as the transition from FM coupling to AFM coupling in small pure manganese clusters with the increase of atom number.[23] In Co_nV_m, average magnetic moment decreases with m increase. When m is small, the opposite sign between local magnetic moment of Co and V reflects antiferromagnetic coupling. When m is large, the magnetic moments are dissipated on V atoms. As we know, bulk state of vanadium is nonmagnetic. And research about pure small vanadium clusters proved their small magnetic moment.[24] This is the reason why AMM decreases with V doped. Dennler et al.[8] studied the magnetic properties of Co−Rh and concluded that Co can induce a remarkable enhancement of the local magnetic moment at the Rh neighbors at low Co concentration. But in our systems, this is not the case. In Co−Mn clusters, the Mn atoms always possess large local magnetic moment (approximately $4.5\mu_B$), whereas in Co−V clusters, Co can induce large local magnetic moment on V only in Corich systems.

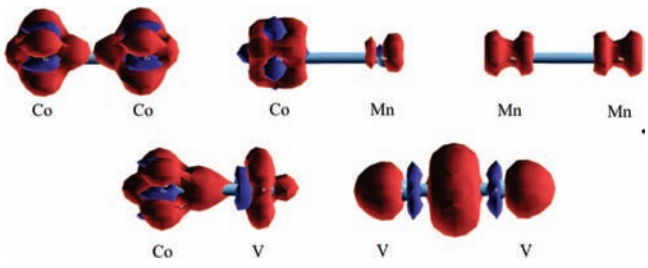

Figure 6. Charge deformation density of Co_2, CoMn, Mn_2, CoV, and V_2.

C. Local Magnetic Moment of Cobalt. In our study Co atoms exist in both systems, so a more detailed observation on local magnetic moment of cobalt may do good for clear understanding of magnetism in clusters. From Mulliken analysis, we show the trends for Co average local magnetic moment (ALMM) in both Co−Mn and Co−V systems in Figure 5.

1. Co−Mn Systems. The Co ALMM of Co−Mn clusters show diverse phenomenon: when Mn proportion is less than 30%∼50% (two dashed lines), for small clusters the ALMM increases, whereas for larger clusters, it has a small decreasing trend; but when the proportion goes above 50%, ALMM decreases fast with Mn proportion increasing.

2. Co−V Systems. In the V doped cobalt clusters, Co ALMM decreases in a nearly linear way, except in Co_2V_3 where the magnetic moment of Co atoms is quenched. This exception may be attributed to its special structure: it is a trigonal bipyramid and the Co atoms lie on two apexes. Three vanadium atoms interact with each cobalt atom, which may lead to annihilation of cobalt's local magnetic moment.

3. Explanation. For transition metal clusters, spin polarization is mainly attributed to the localization of d electrons. In general, there are two possible reasons which can induce Co ALMM: one is charge transfer into 3d orbitals, and the other is the delocalization of 3d electrons. As shown below, these two reasons are responsible to Co−Mn and Co−V systems, respectively.

a. 3d Occupation. The phenomenon in Co−Mn is due to the large amount of charge transfer from Co 4s and Mn atoms to Co 3d orbitals. It decreases the Hund holes, therefore the

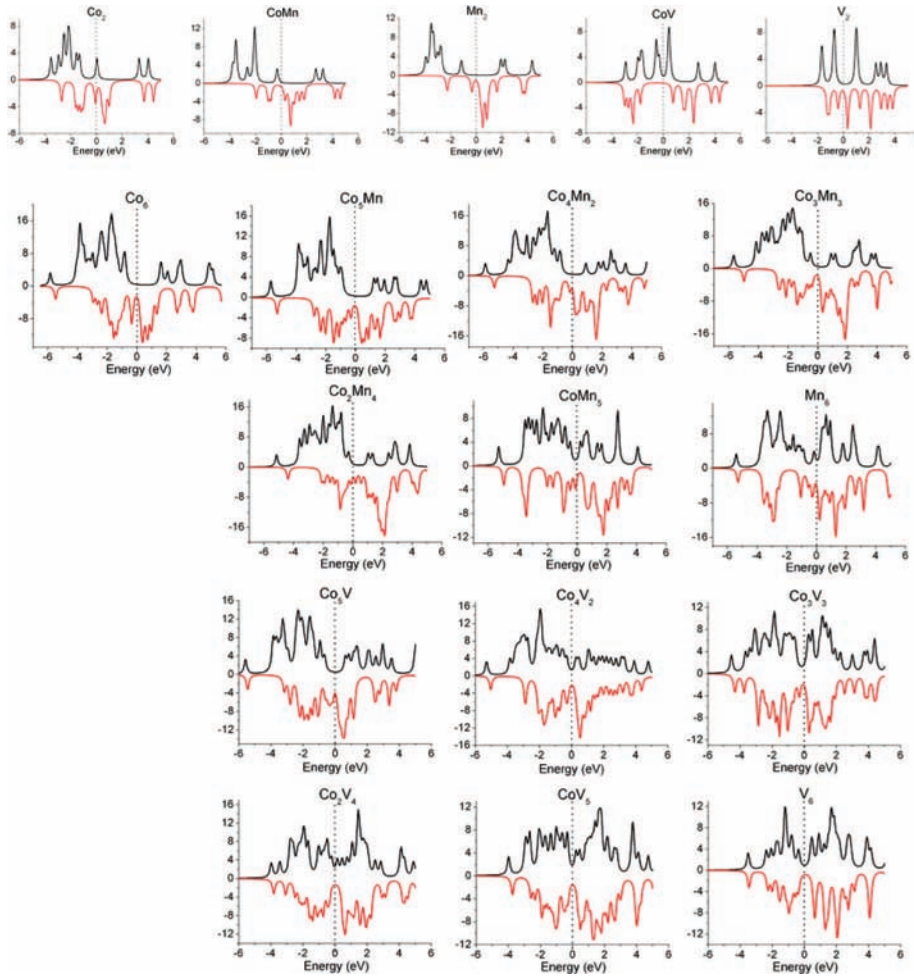

Figure 7. DOS of Co_nTM_m (TM = Mn and V, $m + n = 2$ and 6).

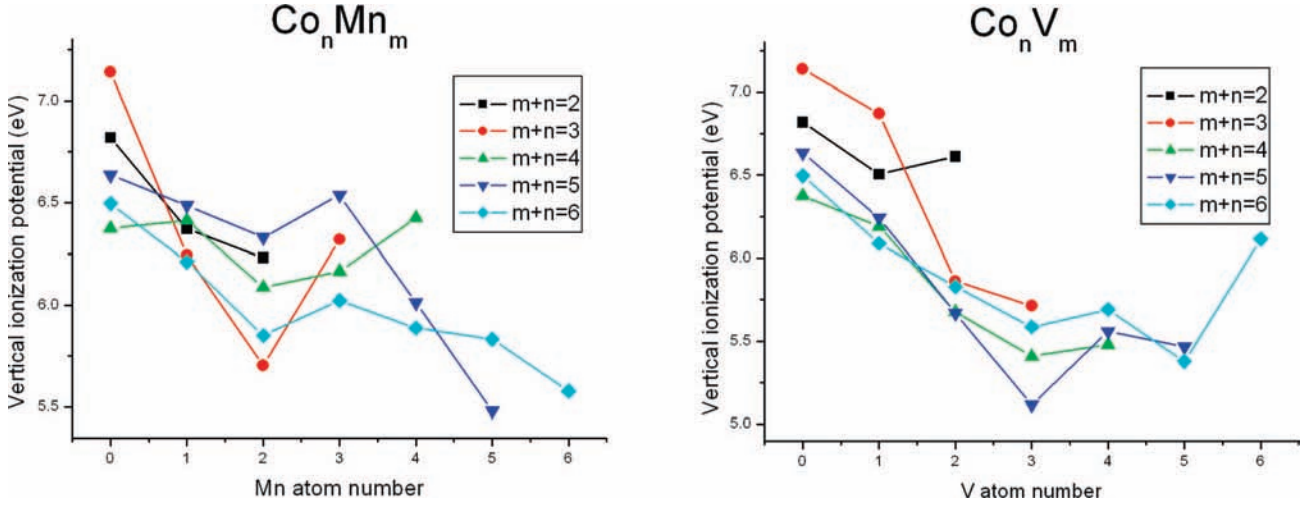

Figure 8. Vertical ionization potential of Co_nTM_m (TM = Mn and V, $m + n \leq 6$).

magnetic moment of cobalt is reduced. This can be reflected from the data of the 3d electron population of cobalt listed in Table 3, where the Co 3d magnetic moment changes by about $0.4\mu_B$ from Co_4 to $CoMn_3$, and the 3d electron number changes by 0.33.

On the other hand, the data of the Co 3d occupation in Co_nV_m as listed in Table 4 show a different behavior: the Co 3d magnetic moment changes by 0.7 μ_B from Co_4 to CoV_3, but the 3d population just changes by 0.3. Therefore, charge transfer solely can not explain the decrease of Co 3d magnetic moment in Co−V clusters. Past research on small Co−V clusters[28] attributed the significant reduction of cobalt ALMM to the electronic redistribution in the various molecular orbitals (MOs), contrary to the atomic orbital (AO) distribution of free atoms. In another words, this is the delocalization of Co 3d electrons, and we will discuss it below.

b. Deformation Density. To have a clear view of how the Mn and V have interaction with Co, the deformation density of each dimer is presented in Figure 6, which is defined as the total charge density with the density of the isolated atoms subtracted.

In these graphs, the isovalue is set as 0.1 e/Å^3. The red area means that when two atoms form a cluster, the charge density increases, while the blue area corresponds to charge density decrease. When Co forms bond with Mn, its 3d localization property is not affected by Mn atom, or even enhanced in some way. On the other hand, the V atoms delocalize 3d electrons to Co. Thus the Hund holes have less ability to spin polarization, so Co 3d magnetic moment decreases, and then ALMM is decreased.

D. Density of States. The photoelectron spectroscopy technology is often used to detect the density of states (DOS) of clusters. To guide further experiment research, we plot the DOS of 2-atom and 6-atom clusters in Figure 7. From these graphs, we find some interesting phenomenon: for Co−Mn clusters, although the magnetic moment drops when Mn proportion becomes large, the shapes of the alpha and beta DOS are always quite different. This is due to the fact that each atom still has local magnetic moment, and some of them are antiferromagnetically coupled. On the other hand, for Co−V clusters, with the increase of V atoms the magnetic moment drops, and at the same time the shapes of alpha and beta DOS become nearly perfectly matching. This is explained as all the atoms have small spin polarization.

E. Vertical Ionization Potential. The vertical ionization potential (IP) is calculated as the energy of cluster with charge +1 minus the energy of neutral cluster. It is an important property for clusters and can be compared with experiment, and we plot it in Figure 8. The vertical IP of all the clusters are between 5 and 7.5 eV. In general there is a decreasing trend of IP with increase of doping, but it is far from monotonic. This trend is also seen in the experimental work by Koretsky et al.[29] on vertical IP of Co_nMn_m ($8 \leq m + n \leq 31$).

V. Conclusion

In this article, we carry out systematic DFT study for bimetallic Co_nMn_m and Co_nV_m ($m + n \leq 6$) clusters. We get the ground states of these clusters. In these structures, the trends for Co/V to congregate in Co_nMn_m/Co_nV_m clusters are found, and they can be explained by the bond energy order. Average binding energy increases/decreases with Mn/V doping, respectively. Total magnetic moments are enhanced by doped Mn when Mn atoms are separated by cobalt, and reduced when Mn atoms interact with each other; while they decrease with doped V. Careful examinations of cobalt average local magnetic moment indicate that the reason for magnetic moment change of cobalt is charge transfer in Co_nMn_m and is 3d delocalization in Co_nV_m. Vertical ionization potential and DOS are shown to guide further experiments.

Acknowledgment. We thank Shuanglin Hu, Er-Jun Kan, Jun Dai, and Fu Chen for helpful discussions. This work is supported by the National Natural Science Foundation of China (20603032, 50721091, 50731160010), by National Key Basic Research Program under Grant No. 2006CB922004, by a Foundation for the Author of National Excellent Doctoral Dissertation of P. R. China (2007036), by the Shanghai Supercomputer Center, the USTC-HP HPC project, and the SCCAS.

References and Notes

(1) Bucher, J. P.; Douglass, D. C.; Bloomfield, L. A. *Phys. Rev. Lett.* **1991**, *66*, 3052.
(2) Apsel, S. E.; Emmert, J. W.; Deng, J.; Bloomfield, L. A. *Phys. Rev. Lett.* **1996**, *76*, 1441.
(3) Cox, A. J.; Louderback, J. G.; Bloomfield, L. A. *Phys. Rev. Lett.* **1993**, *71*, 923.
(4) Reddy, B. V.; Khanna, S. N.; Dunlap, B. I. *Phys. Rev. Lett.* **1993**, *70*, 3323.
(5) Vega, A.; Dorantes-Dávila, J.; Pastor, G. M.; Balbás, L. C. *Z. Phys. D* **1991**, *19*, 263.
(6) Muñoz-Navia, M.; Dorantes-Dávila, J.; Pastor, G. M. *J. Phys.: Condens. Matter* **2004**, *16*, S2251.
(7) Dennler, S.; Morillo, J.; Pastor, G. M. *Sur. Sci.* **2003**, *532*, 334.
(8) Dennler, S.; Morillo, J.; Pastor, G. M. *J. Phys.: Condens. Matter* **2004**, *16*, S2263.
(9) Guirado-López, R.; Villaseñor-González, P.; Dorantes-Dávila, J.; Pastor, G. M. *Eur. Phys. J. D* **2003**, *24*, 237.
(10) Aguilera-Granja, F.; Vega, José Rogan, A.; Andrade, X.; García, G. *Phys. Rev. B* **2006**, *74*, 224405.
(11) Yin, S.; Moro, R.; Xu, X.; de Heer, W. A. *Phys. Rev. Lett.* **2007**, *98*, 113401.
(12) Ma, Q.-M.; Xie, Z.; Wang, J.; Liu, Y.; Li, Y.-C. *Phys. Lett. A.* **2006**, *358*, 289.
(13) Mpourmpakis, G.; Froudakis, G. E. *Phys. Rev. B.* **2005**, *72*, 104417.
(14) Rodríguez-López, J. L.; Aguilera-Granja, F.; Michaelian, K.; Vega, A. *Phys. Rev. B* **2003**, *67*, 174413.
(15) Datta, S.; Kabir, M.; Ganguly, S.; Sanyal, B.; Saha-Dasgupta, T.; Mookerjee, A. *Phys. Rev. B* **2007**, *76*, 014429.
(16) Kabir, M.; Mookerjee, A.; Kanhere, D. G. *Phys. Rev. B* **2006**, *73*, 224439.
(17) Gutsev, G. L.; Mochena, M. D.; Bauschlicher, C. W., Jr *J. Phys. Chem. A* **2006**, *110*, 9758.
(18) Rao, B. K.; Ramos de Debiaggi, S.; Jena, P. *Phys. Rev. B* **2001**, *64*, 024418.
(19) Delley, B. *J. Chem. Phys.* **1990**, *92*, 508. Delley, B. *J. Chem. Phys.* **2000**, *113*, 7756. DMol^3 is available from Accelrys.
(20) Perdew, J. P.; Burke, K.; Ernzerhof, M. *Phys. Rev. Lett.* **1996**, *77*, 3865.
(21) Baerends, E. J.; Branchadell, V.; Sodupe, M. *Chem. Phys. Lett.* **1997**, *265*, 481.
(22) Kant, A.; Strauss, B. *J. Chem. Phys.* **1964**, *41*, 3806.
(23) Bobadova-Parvanova, P.; Jackson, K. A.; Srinivas, S.; Horoi, M. *J. Chem. Phys.* **2005**, *122*, 014310.
(24) Sun, H. Q.; Luo, Y. H.; Zhao, J. J.; Wang, G. H. *Phys. Stat. Sol. B* **1999**, *215*, 1127.
(25) Calaminicia, P.; Köster, A. M. *J. Chem. Phys.* **2001**, *114*, 4036.
(26) Langridge-Smith, P. R. R.; Morse, M. D.; Hansen, G. P.; Smalley, R. E.; Merer, A. J. *J. Chem. Phys.* **1984**, *80*, 593.
(27) Spain, E. M.; Morse, M. D. *J. Phys. Chem.* **1992**, *96*, 2479.
(28) Andriotis, A. N.; Mpourmpakis, G.; Froudakis, G. E.; Menon, M. *J. Chem. Phys.* **2004**, *120*, 1–1901.
(29) Koretsky, G. M.; Kerns, K. P.; Nieman, G. C.; Knickelbein, M. B.; Riley, S. J. *J. Chem. Phys. A* **1999**, *103*, 1997.
(30) Grönbeck, H.; Rosén, A. *J. Chem. Phys.* **1997**, *107*, 10620.
(31) Ratsch, C. *J. Chem. Phys.* **2005**, *122*, 124302.

JP804188U